CHAPTER 3

DATA ACQUISITION CONSIDERATIONS

3.1 Introduction. The WSR-88D has a number of user-selectable and site-specific data acquisition parameters enabling the user to optimize the acquisition and signal analysis to the particular meteorological situation. Acquisition optimization requirements often present conflicting demands on the system such as where estimate accuracy improvements require longer dwell times but the lifetime of meteorological features requires fast temporal sampling and thus short dwell times. Usually, the actual acquisition scheme will be a compromise between several conflicting requirements so as to satisfy the critical meteorological requirements such as temporal sampling and spatial resolution.

3.2 Temporal and Spatial Sampling. The temporal sampling time, i.e., the volume throughput rate, is driven by two general considerations: 1) the rate of change with time of the general information content of the meteorological characteristics being examined and 2) the lifetime of the weather event to be detected.

One of the more descriptive measures of general information change in the meteorology is correlation, as either a function of time or space, since this provides a measure of how much the process is changing. Values of correlation close to unity imply small changes from sample to sample with little new information. Values of correlation close to zero imply large changes from sample to sample with new information. For example, for purposes of estimate variance reduction with Gaussian statistics, a correlation of 0.15 means that about 25 percent of the information is redundant, a correlation of 0.5 means that about 50 percent is redundant, and a correlation of 0.9 means that about 80 percent is redundant. Measured values of the correlation of reflectivity and mean velocity are shown in Figure 3-1. Two general conclusions that can be drawn from the given behavior are: the mean velocity field is more persistent in time than the reflectivity field, and both reflectivity and mean velocity are significantly correlated (>0.3) with sampling intervals less than about 9 minutes. For the approximately Gaussian behavior exhibited by the correlation, this implies a significant information redundancy. Thus, temporal sampling intervals less than about 9 minutes will enable recovery of most information concerning total precipitation, storm type, mean motion, and other general characteristics of the system.

In most cases, the more stringent temporal sampling requirement will be imposed by detection of a weather event. Some representative events and approximate life times are tabulated in Table 3-1. It is seen that detection of the shorter life phenomena requires temporal sampling at about 5-minute intervals.

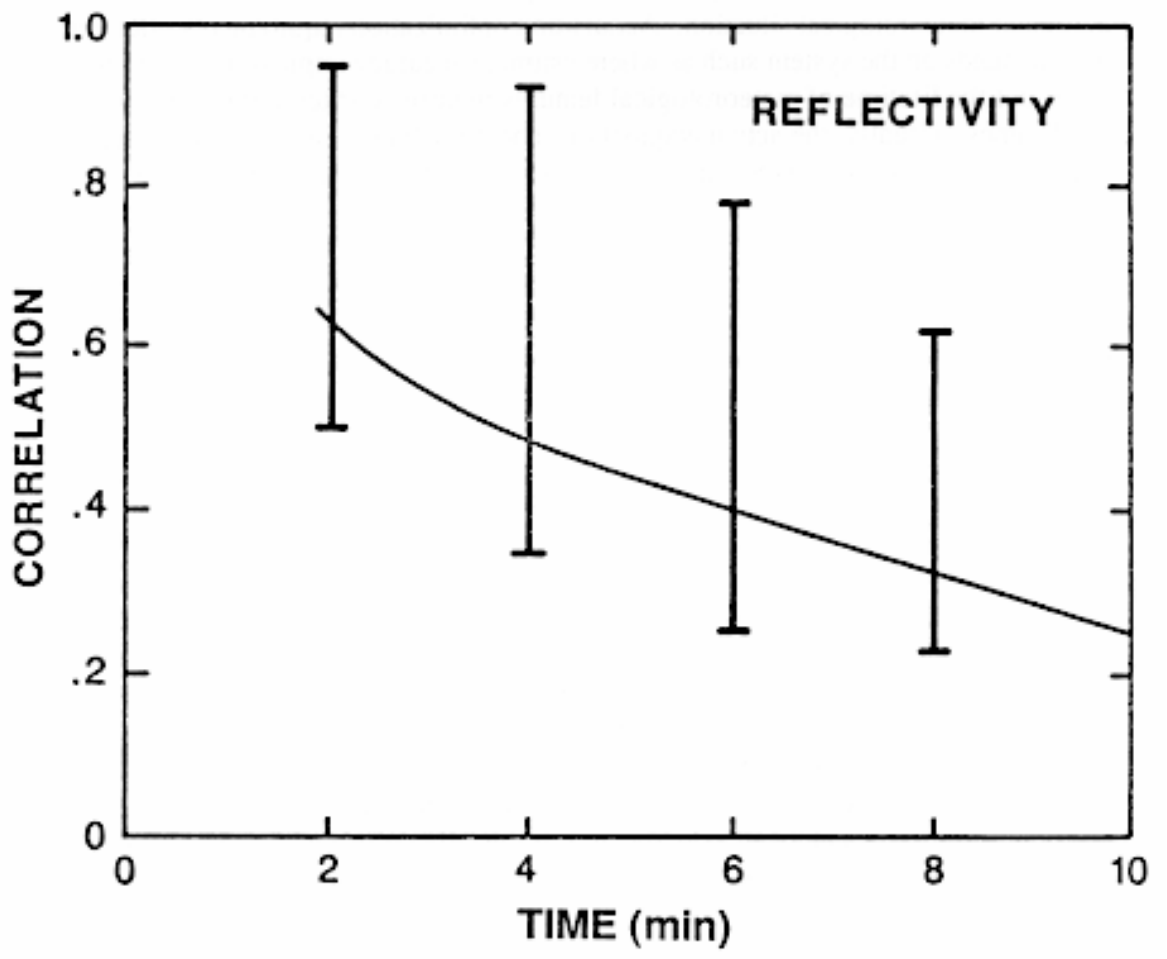

Figure 3-1a
Autocorrelation of Reflectivity with Time

Autocorrelation provides a measure of time rate of change of the measured parameter, i.e., how much new information is available as a function of the sampling rate. Vertical bars bracket the range of values reported for a variety of meteorological situations.

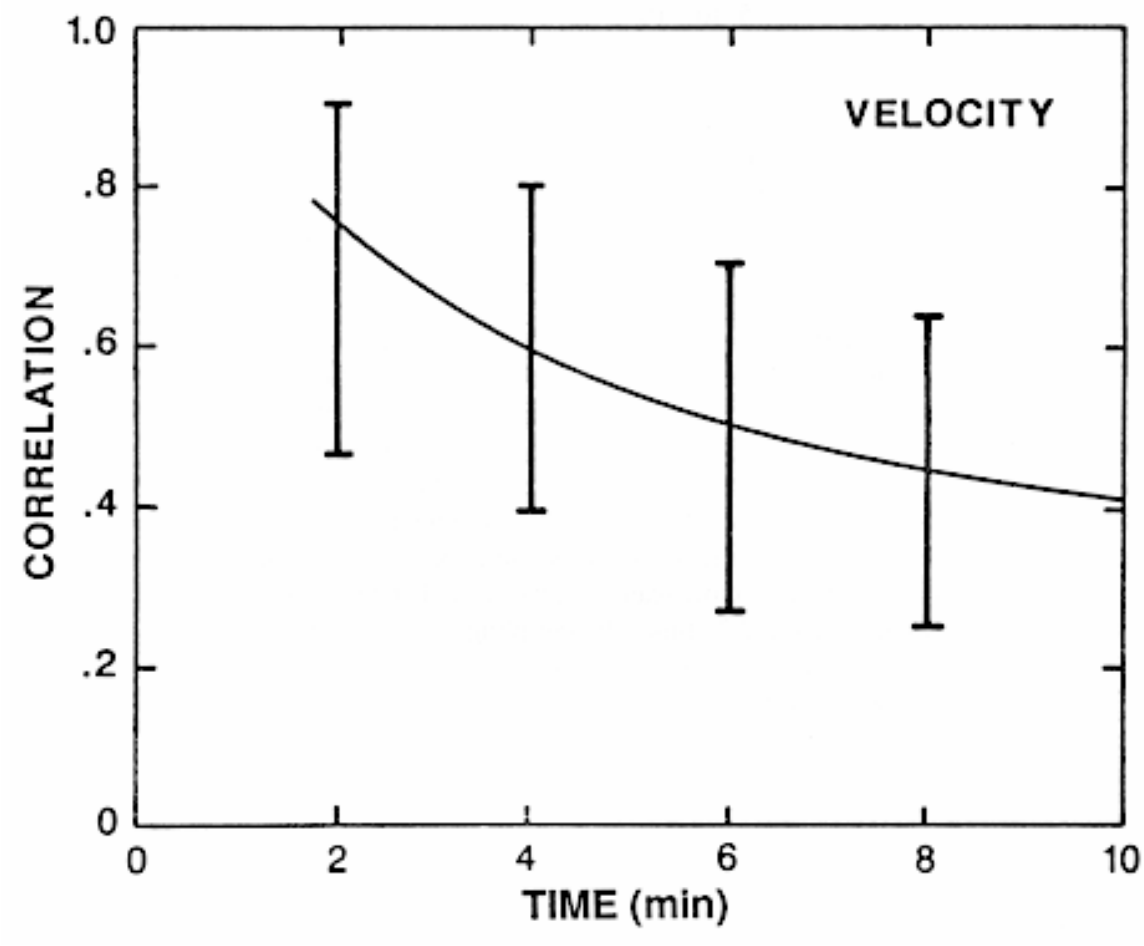

Figure 3-1b
Autocorrelation of Mean Radial Velocity with Time

Autocorrelation of mean radial velocity for a given lag is higher than reflectivity implying more redundancy for a given sampling rate. Vertical bars bracket the range of values reported for a variety of meteorological situations.

Spatial sampling requirements can also be described in terms of the general field correlation and spatial scale of weather events. The general behavior of the correlation with distance is similar to Figure 3-1 with correlation lengths (i.e., ~0.3) of about 600 m (1969 ft) for both reflectivity and velocity. However, as in the case for temporal sampling, the driving criterion is usually detection of weather events. Some common events and associated scales are also given in Table 3-1. Obviously, resolution scales of a few km must be maintained to detect the smaller events.

Table 3-1
Temporal and Spatial Sampling

Weather Event	Temporal Scale (mins)	Spatial Scale (km/nm)
Heavy Rain	5 to 60	~10/5.4
Hail	5 to 10	~5/2.7
Wind Features		
Gust Front	5 to 30	~1 x 30/0.54 x 16.2
Shear Zone	10 to 30	~1 x 10/0.54 x 5.4
Mesocyclone	15 to 60	~4/2.2 (Signature)
Convergence/ Divergence	10 to 60	~5 x 20/2.7 x 10.8 (Signature)

The resolution maintained by the polar grid associated with the basic radar data acquisition is proportional to the sampling interval (but is not, by the conventional definition, numerically equal to the sampling interval). Acquiring data by averaging over a finite interval (in either time or space or both) and outputting the average as representative of the value over the acquisition interval has the spatial transfer associated with the "zero order hold," i.e., each cell has a data value equal to the average over the range and angle equal to the cell dimensions and zero otherwise. The signal amplitude transfer (ordinate) as a function of the radial periodicity (abscissa) of the field is shown in Figure 3-2. The half power cutoff scale, i.e., the scale that has an amplitude reduction to 70% of the large-scale value, is about 2.27 times the sampling or averaging interval. Note also the sharp cutoff of the transfer function for scales less than the half-power value. Features having a scale less than the cutoff will not be retained in the data. For the WSR-88D, this means that meteorological parameters less than 2.27 times the range averaging interval will not be retained in the data. The range averaging interval for reflectivity is 1 km (0.54 nm) out to 230 km (124 nm) and is 2 km (1.1 nm) beyond 230 km (124 nm). The range averaging interval for velocity and spectrum width is 0.25 km (0.13 nm) out to 230 km (124 nm).

A similar derivation can be made for resolution in the azmuthal direction of the polar grid. The half power cutoff is again 2.27 times the angular sampling interval, $\Delta\theta$, with a spatial cutoff length given by $r \sin \Delta\theta$. The cutoff scale in the azmuthal direction is shown in Figure 3-3.

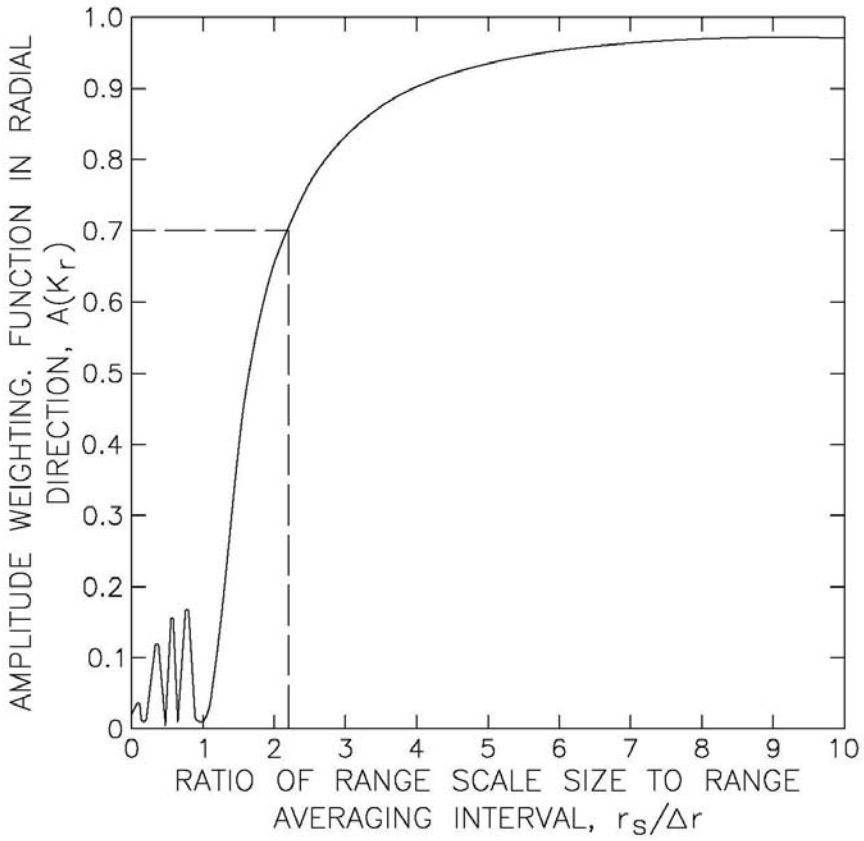

Figure 3-2
Meteorological Field Spatial Scale Amplitude Weighting Function

Transfer for sinusoidal variations with period, r_s, due to averaging over an interval, Δr. Note that variations having a period less than twice the averaging interval are not retained in the average.

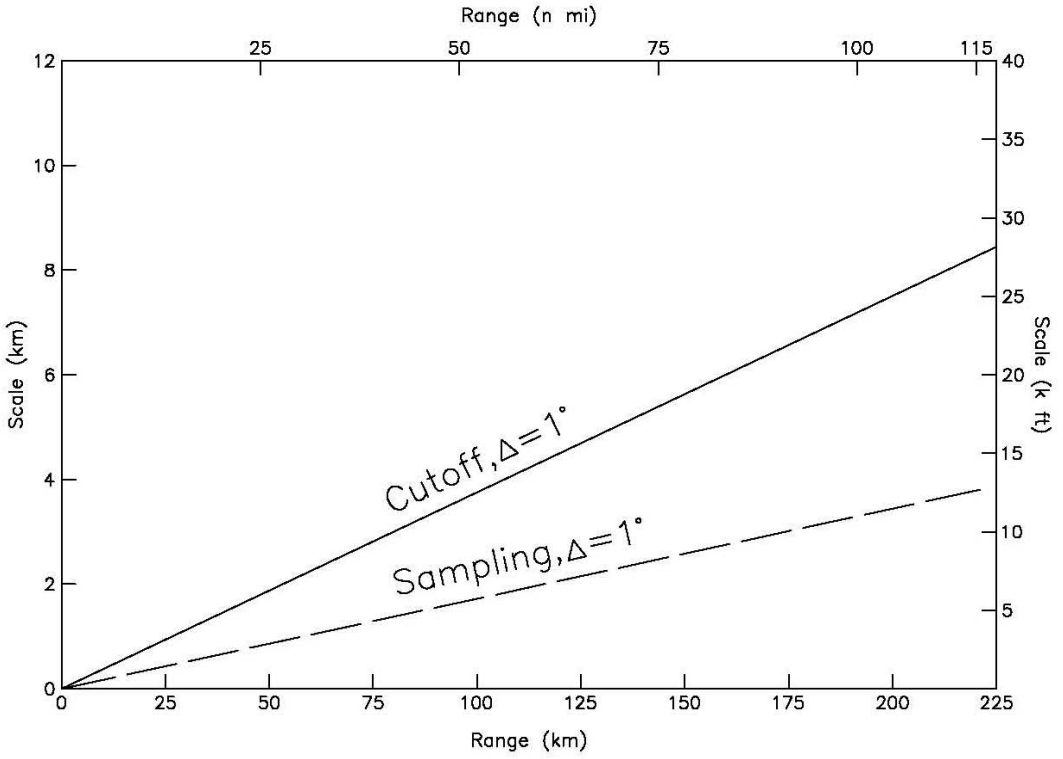

Figure 3-3
Sampling and Cutoff Scale Length

Cutoff scale for radar resolution in the azmuthal direction of the polar grid.

In summary, the sampling density limits the meteorological scale that can be resolved by the radar in that dimension. The cutoff scales are: 2.27 Δr (Δr is the range sampling interval) in the radial direction and sin (2.27 $\Delta\theta$) in the angular direction. For the WSR-88D base data, the range cutoff scale is 500 m (1640 ft) for radial velocity and spectrum width [sampled at a 250 m (820 ft) interval] and 2.27 km (1.2 nm) for reflectivity [sampled at 1 km (0.54 nm)]. Cutoff scales in the azimuth and elevation directions are range dependent and equal to r sin (2.27 $\Delta\phi$), where $\Delta\phi$ is angular increment. For 1° samples this reduces to about $4(10^{-2})r$.

Polar grid density and data throughput rate (i.e., antenna rotation rate), by determining the number of radar samples available for processing, determine the performance of the radar system in areas such as accuracy of the estimates and magnitude of the clutter suppression.

Signal coherency merely requires that the radar Nyquist co-interval, $\pm 2v_a$, be "large" compared to input signal spectrum width. This is interpreted as being such as to maintain the majority of input widths in the linear region of mean velocity estimates of performance, i.e., below the inflection point of the performance curve shown in Figure A-6.

From the cumulative distribution of spectrum widths given in Figure 3-4, it is seen that the 95-percentile spectrum width in convective storm systems (generally a worst case) is about 10 ms^{-1} (19 kts). From Figure A-6 it is seen that signal coherency and, thus, estimate accuracy deteriorate rapidly for input spectrum greater than 14 ms^{-1} (27 kts) for a Nyquist velocity of 31.5 ms^{-1} (62 kts), 11 ms^{-1} (22 kts) for v_a=25.6 ms^{-1} (50 kts), and 10 ms^{-1} (19 kts) for v_a = 22.5 ms^{-1} (44 kts). Thus, spectrum coherency is maintained for most signals at all PRTs of the WSR-88D and the variation of estimator accuracy and suppression is nominal (less than 10% of any parameter). A more important aspect of PRT selection is to minimize range folding and velocity aliasing.

Range folding and velocity aliasing are other examples of conflicting operational criteria. Minimizing velocity aliasing requires a high Nyquist velocity (high PRF) while minimizing range folding requires a low Nyquist velocity (low PRF). The automatic PRF selection of the WSR-88D is based on minimizing range folding, i.e., the system selects that PRF (from the choices available) that will minimize the area obscured by overlaid echoes. This provides maximum data recovery but has two drawbacks.

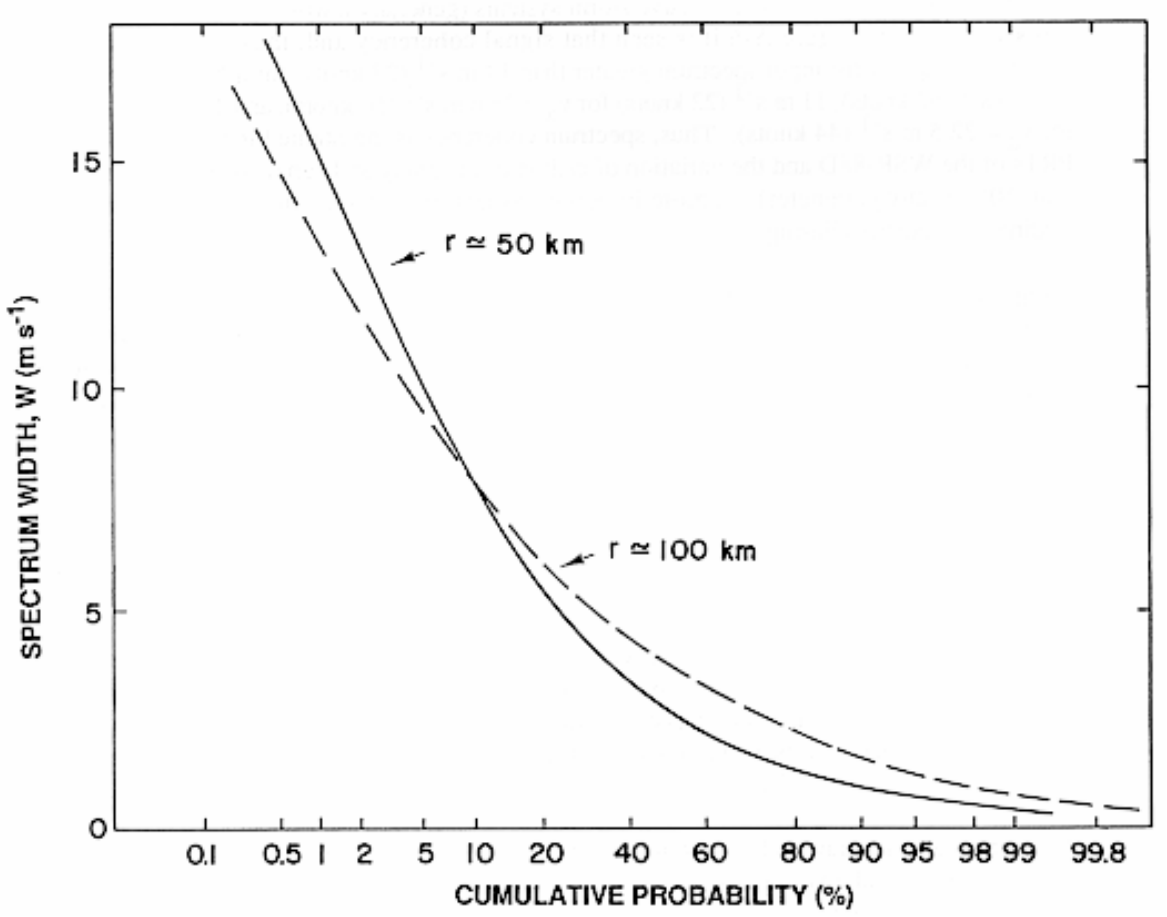

Figure 3-4
Cumulative Probability for Convective Storms

The probability that the spectrum width is larger than the ordinate value, for convective storms at 50 km and 100 km. The median value, that value for which half of the widths are larger and half the widths are smaller, is about 4 ms^{-1}.

Minimizing the area obscured by overlaid echoes will tend to utilize the maximum system PRT and thus the minimum Nyquist velocity that, in turn, will increase the velocity aliasing for a given situation. From the velocity magnitude percent of occurrence shown in Figure 3-5 it is seen that some aliasing will occur at any of the PRTs available (without using Volume Coverage Pattern (VCP) 121 and the Multiple PRF Dealiasing Algorithm, MPDA). It is also evident from the steep slopes of the velocity distribution that velocity aliasing will change rapidly with a change in Nyquist co-interval. For the Nyquist co-intervals available and without reliance on an alternate VCP such as VCP 121, the percent aliasing will increase about an order of magnitude as the Nyquist co-interval is decreased from $\pm$31 ms^{-1} to $\pm$22.5 ms^{-1} ($\pm$60 to $\pm$44 kts). Without using VCP 121 (and the MPDA), there will be situations where the user must assume manual control of the PRT in order to achieve optimum data recovery. On the other hand, the user can opt to use VCP 121 to minimize range overlaid echo while at the same time minimizing velocity aliasing. In fact, this is the preferred solution. Another occasional drawback of minimizing the area obscured is loss of high-interest data due to the minimal residual obscuration. In this case the user will again need to assume manual control and select the PRT such as to clear the region of interest. But even this occurrence will be greatly minimized through use of VCP 121.

In summary, the WSR-88D estimate accuracy and clutter suppression performance, as a function of antenna speed for a 1° azimuth sampling, is shown in Figure 3-6. Accuracy of the estimates and suppression is also dependent on the transmitter PRT through its influence on signal coherency.

3.3 Data Recovery by Ground Clutter Suppression. Prior to calculation of reflectivity, R, velocity, v, or spectrum width, W, return signals from ranges within the radar ground pattern are passed through devices that remove most of the signal. These clutter suppressors take advantage of statistical properties returned from stationary or clutter targets, which are usually different from the meteorological signals, in order to reject the clutter. The two most important properties are mean Doppler velocity and spectrum width or signal correlations.

Ground clutter is usually stationary, has near zero mean Doppler velocity, and has a small dispersion or spectrum width. Typical clutter spectrum widths range from <0.1 ms^{-1} (<0.2) to about 0.5 ms^{-1} (1). This is much smaller than the widths of most meteorological signals that have median values ranging from about 1 ms^{-1} (2 kts) for snow and stratiform rain to about 4 ms^{-1} (8 kts) for convective storms.

Thus, as can be visualized from the transfers shown in Figure 3-7, a band-reject filter with a notch around zero velocity will reject most of the clutter without seriously affecting the meteorological signal so long as the mean velocity of the reflecting particles is several times the notch width.

The WSR-88D Doppler channel clutter suppressor is equipped with selectable notch width ranging from about 0.5 ms^{-1} to 2.0 ms^{-1} (1 to 4 kts) with the filter controlled by a site selectable clutter map. In the Doppler channel, the unit will deliver a peak suppression of about 50 dB and an average suppression of about 40 dB.

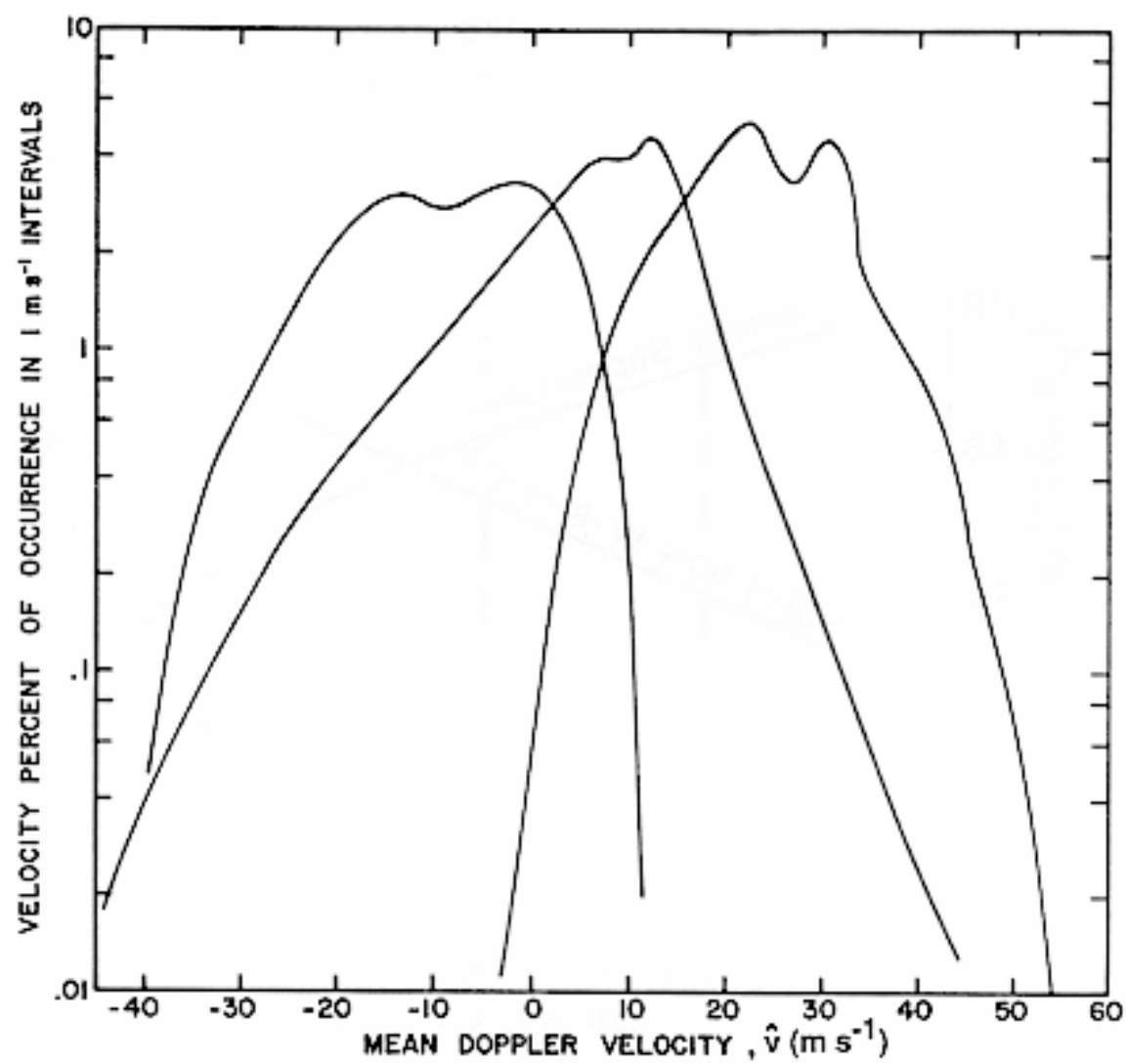

Figure 3-5
Histograms of Velocity for Three Tornadic Storms

The storm translation velocity has been removed.

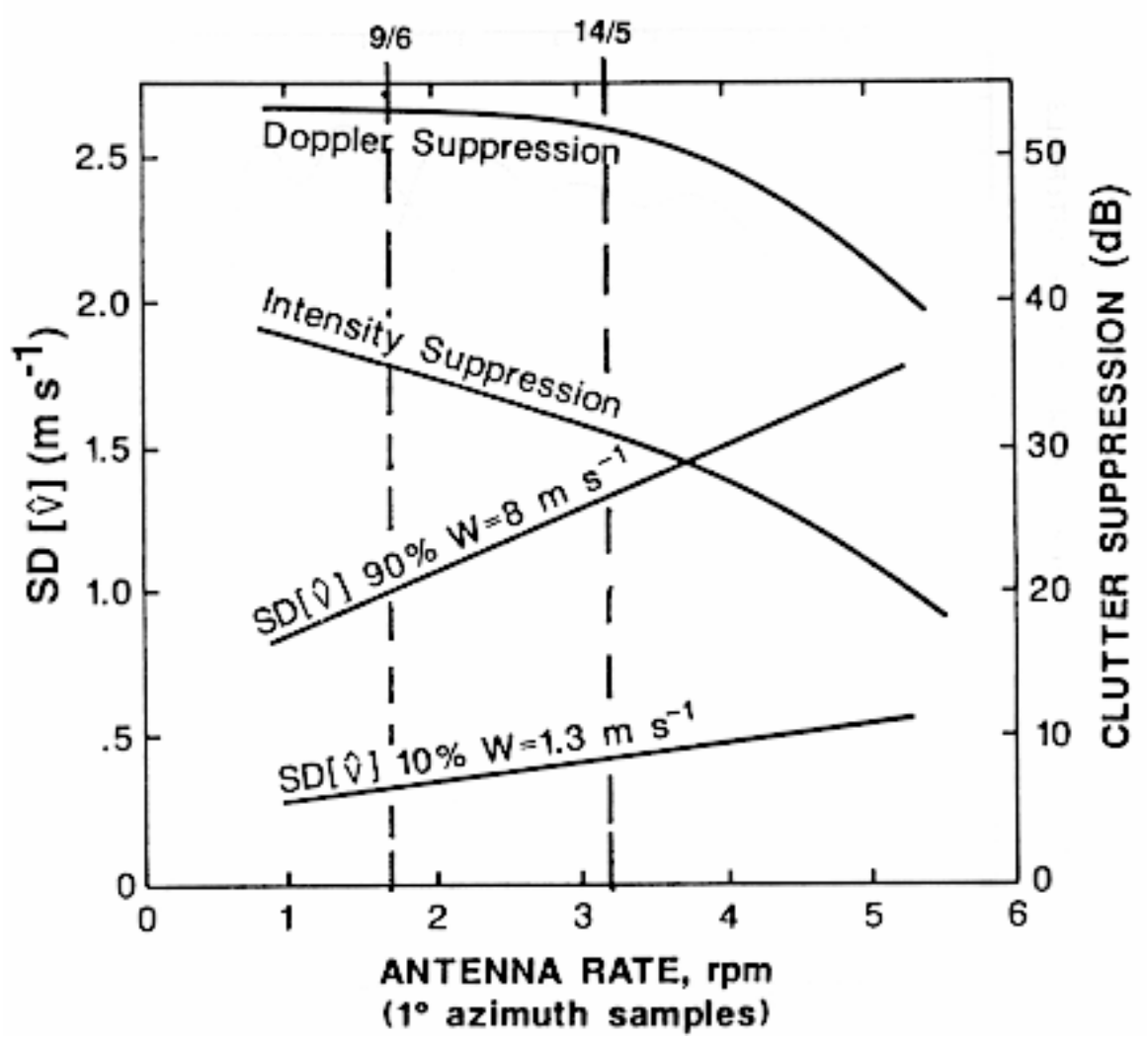

Figure 3-6
Standard Deviations of the Velocity Estimates and Ground Clutter Suppression

Performance as a function of antenna speed with a one degree azimuth sample. Vertical lines intersect performance at throughput rates of 9 unique elevations in 6 minutes and 14 unique elevations in 5 minutes. Spectrum widths, W, of 1.3 ms^{-1} and 8 ms^{-1} are the 10 and 90 percentile widths expected in convective storms.

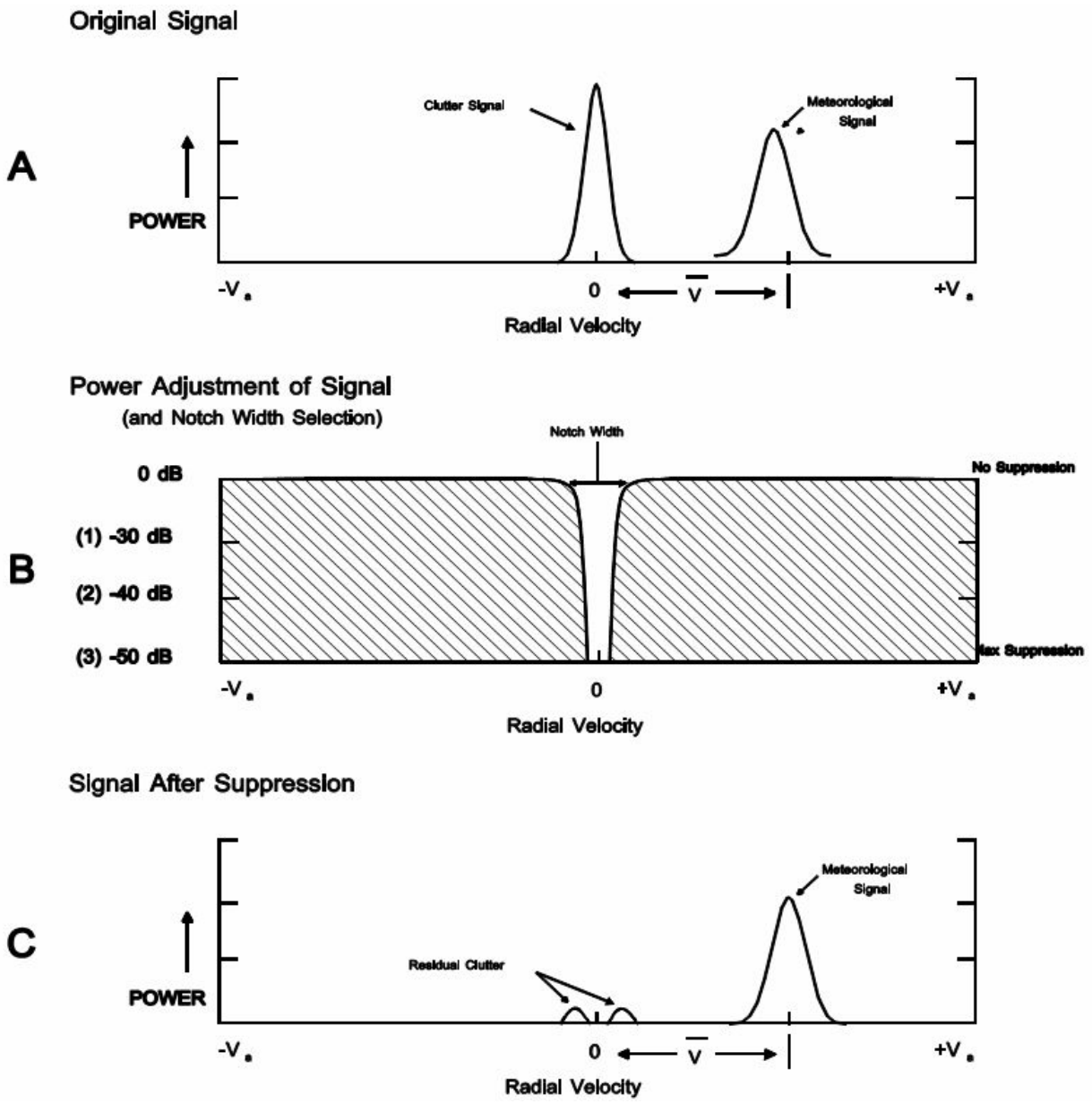

Figure 3-7
Simple Conceptual Model of Legacy Clutter Filter

(A) A depiction of the input power for a given range bin. The clutter signal has a radial velocity centered around zero and the meteorological signal is offset from zero due to its radial velocity. (B) Represents the clutter filter with a notch width centered on zero radial velocity. The scale represents the amount of power reduction, from 0 dB (no power reduction) to -50 dB (maximum power reduction), applied within the notch width. (C) A diagram of the resulting power after the algebraic addition of the signal from A and the power reduction factor from B (A+B=C). From Chrisman and Ray (2005).

Efficiency of the clutter removal depends on the notch depth and the relative width of the notch and clutter signal. In general, the wider the notch, the larger the clutter rejection is. However, in the Doppler channel, wider notches result in larger minimum velocities that will be passed unaffected. If the meteorological signal has a mean velocity at or near zero, a significant portion of this signal will also be rejected. The magnitude of rejection is generally less for the meteorological signal than a clutter signal of comparable strength since the width of the meteorological signal is usually much larger than the notch width. However, in situations where the width of the meteorological signal is small, such as snow or stratiform rain, rejection of the meteorological signal along the zero isotach can result in serious spectrum distortion or complete signal loss. This effect is shown in Figure 3-8, which gives the minimum usable velocity as a function of the suppression magnitude.

Another consideration is that residue from a strong clutter signal, in the presence of a weak meteorological signal can produce a significant bias in the signal estimate. Estimates of signal power, mean velocity, and spectrum width are all affected by the residue but the effect on the mean velocity estimate is probably the more important. Bias effects of clutter or clutter residue are shown in Figure 3-9 where it is seen that, if the residue power is 10 dB below the signal power, the maximum bias is about 1 ms^{-1} (2 kts--about the same as the standard deviation of the estimate). If the residue power is within 5 dB of the signal power, the bias is 2.5 ms^{-1} (5 kts) and probably unacceptable.

The clutter suppression in the reflectivity channel is of the same design as the Doppler channel, i.e. a band-reject filter with the notch around zero velocity.

The worst case, i.e., zero mean velocity, intensity estimate bias, as a function of spectrum width, is shown in Figure 3-10 where it is seen that this bias can be appreciable for spectrum widths less than about 2 ms^{-1} (4 kts). For most convective meteorology, the bias is small (less than 1 dB) and can be accounted for with a connection based on the spectrum width associated with the type of meteorological situation.

3.4 <u>Propagation Considerations</u>. In free space, radio waves travel in straight lines. In the Earth's atmosphere, however, electromagnetic waves are generally bent or curved downward due to the variation with height of the index of refraction. Index of refraction here is defined as the ratio of the velocity of propagation in free space to the velocity of propagation in the atmosphere.

Effects of refraction are the introduction of errors in measurement of radar range and elevation angle.

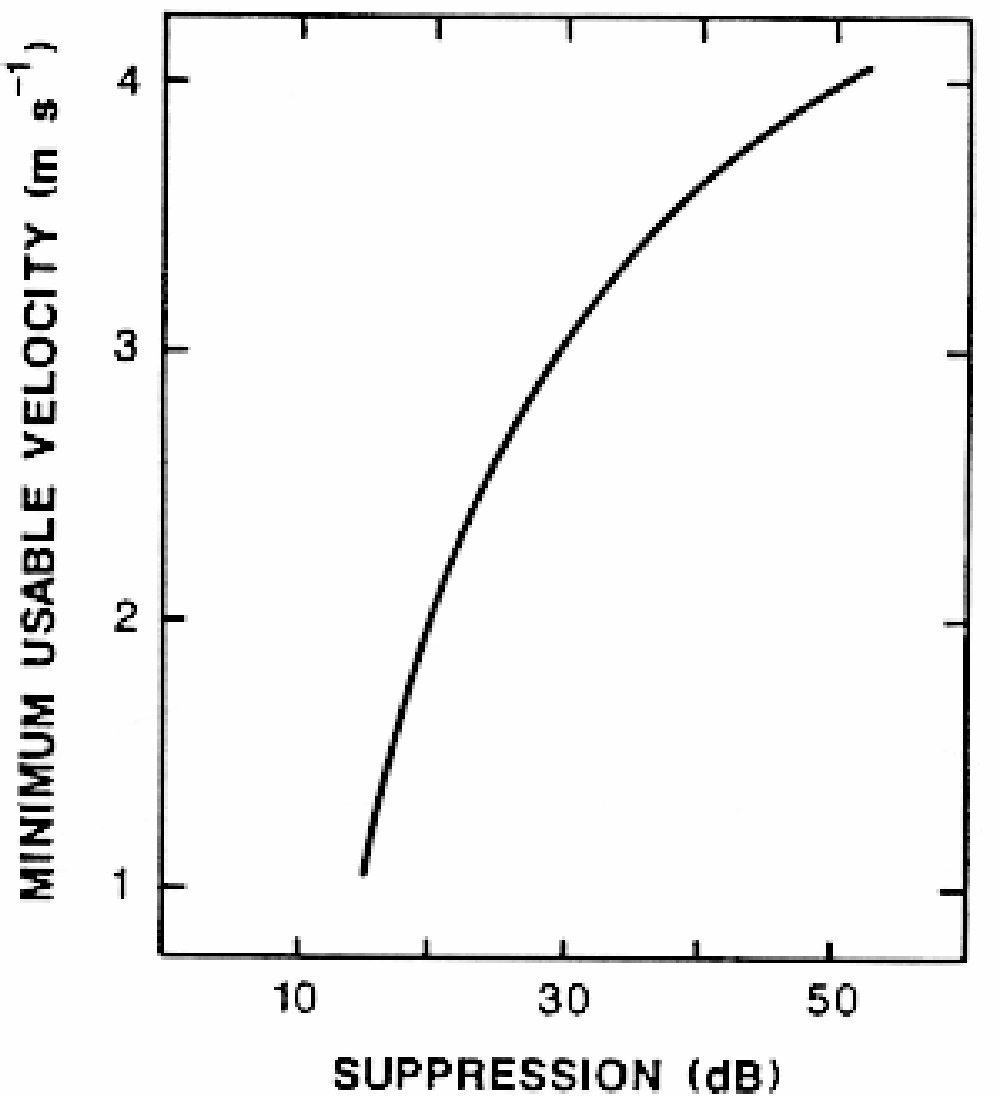

Figure 3-8
Minimum Usable Velocity Due to Suppressor Rejection

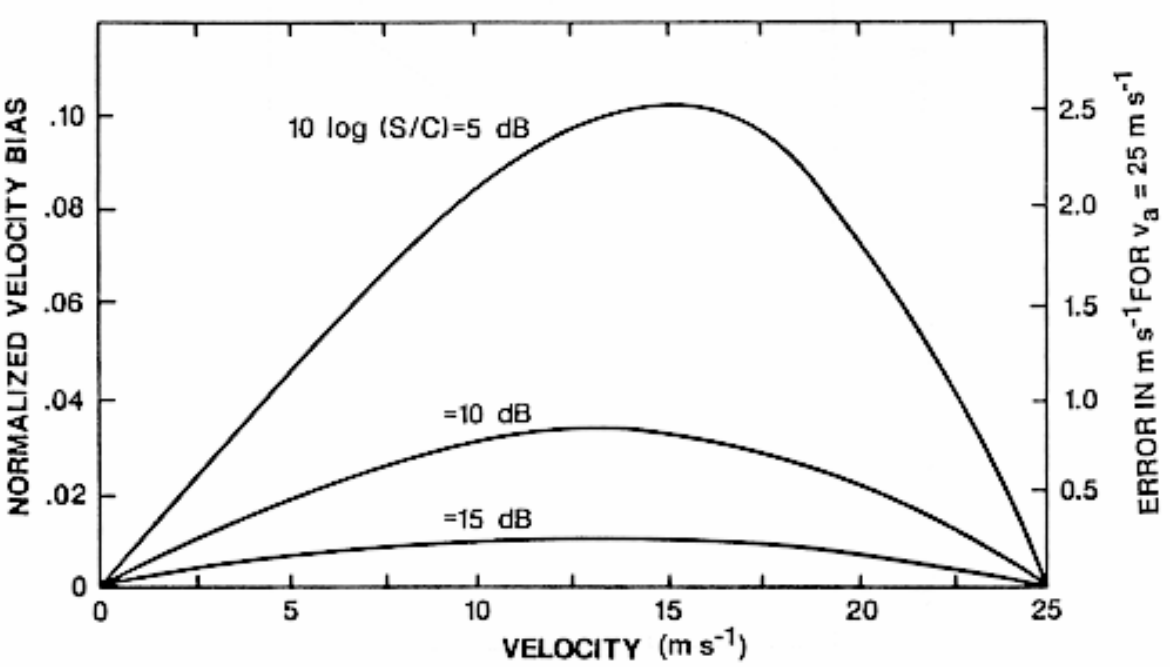

Figure 3-9
Bias of the Velocity Estimate Due to Clutter or Clutter Residue Signal

The bias for unambiguous velocities other than 25 ms^{-1} (13 kts) is equal to the normalized bias times the unambiguous velocity. (S/C = Ratio of Signal Power to Clutter Power)

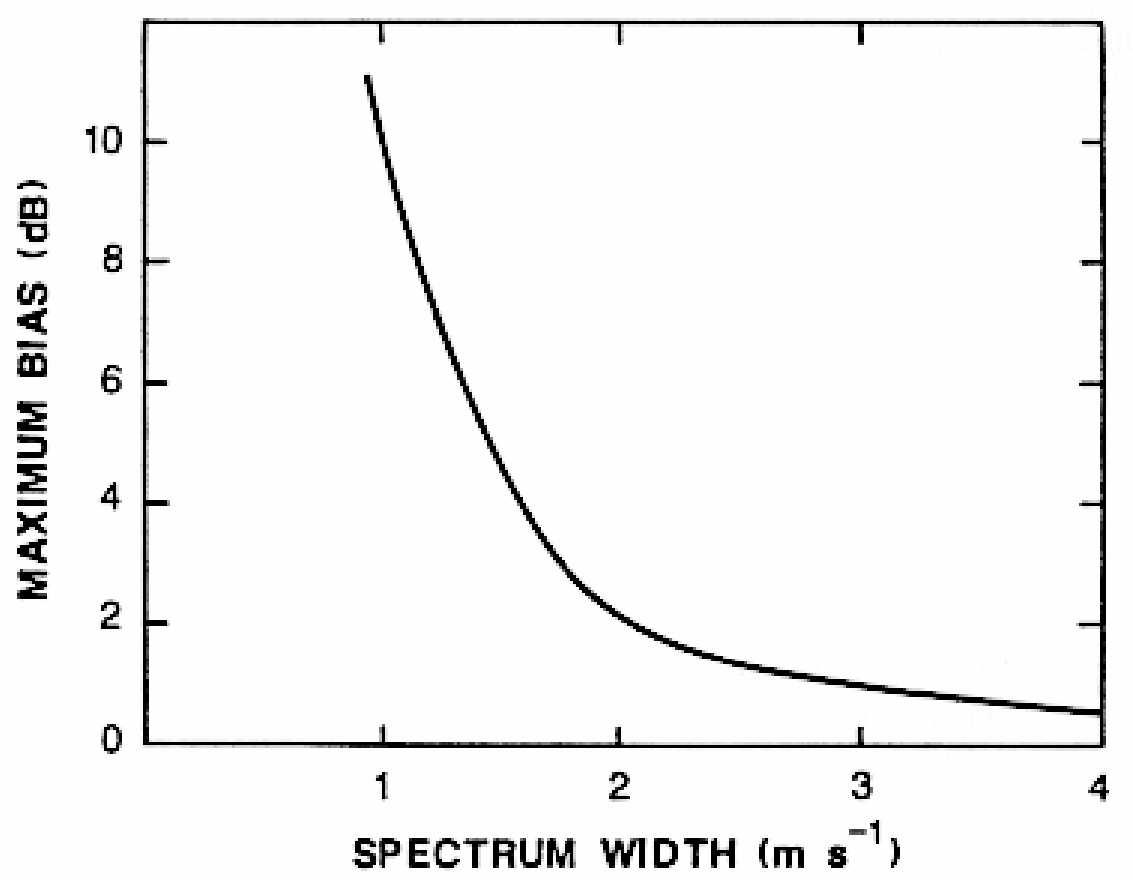

Figure 3-10
Bias of the Reflectivity Estimate Due to Suppressor Rejection as Related to Spectrum Width

Typical spectrum widths (median values) are 4 ms^{-1} (8 kts) for convective storms and 1 ms^{-1} (2 kts) for stratiform rain and snow.

3.4.1 Standard Propagation. At microwave frequencies, the index of refraction of air becomes smaller with decreasing pressure, smaller with decreasing moisture, and larger with decreasing temperature. In the standard atmosphere all three of these variables usually decrease with increasing altitude, but the increase in the index due to decreasing temperature is not sufficient to offset the decrease in the index due to decreasing pressure and moisture. The net result is an almost uniform decrease in refractive index with height up to altitudes of about 7600 m (24,934 ft) under normal conditions resulting in a beam propagation path that is curved downward but with less curvature than the Earth's surface (Figure 3-11).

The index of refraction, *n*, is a function of temperature, pressure, and water vapor and is usually expressed indirectly in a form such as:

$$(n-1)\times 10^6 = N = \frac{77.6P}{T} + \frac{3.73\times 10^5 \varepsilon}{T^2}$$

where:

N = Refractivity (unit of convenience)
T = Air temperature, °K
P = Pressure, millibars
ε = Partial pressure of water vapor, millibars

The first term of the above is the density applicable at all frequencies and the second term accounts for the polarization of water vapor at radio frequencies. Since pressure and water vapor decrease rapidly with height, the index of refraction normally decreases with height. In a standard atmosphere the index decreases at a rate of about $4(10^{-8})$ m^{-1} in altitude. The typical value of n at the Earth's surface is of the order of 1.0003.

The classical method of accounting for refraction in radar-height computations is to replace the actual Earth radius, a, by an equivalent Earth with radius, k • a, and to replace the actual atmosphere by a homogeneous atmosphere in which electromagnetic waves travel in straight lines. It can be shown that the value of k that will result in straight ray paths is:

$$k = \frac{1}{1 + \frac{a}{n}\frac{dn}{dh}}$$

where dn/dh is the rate of change of the refractive index with height. Normally the vertical gradient of the refractive index is negative and, if it is assumed to be constant, the value k is 4/3. Because of its convenience and good accuracy for the normal atmosphere, the 4/3 Earth model is widely used. It is, however, only an approximation that may or may not be satisfactory in all applications.

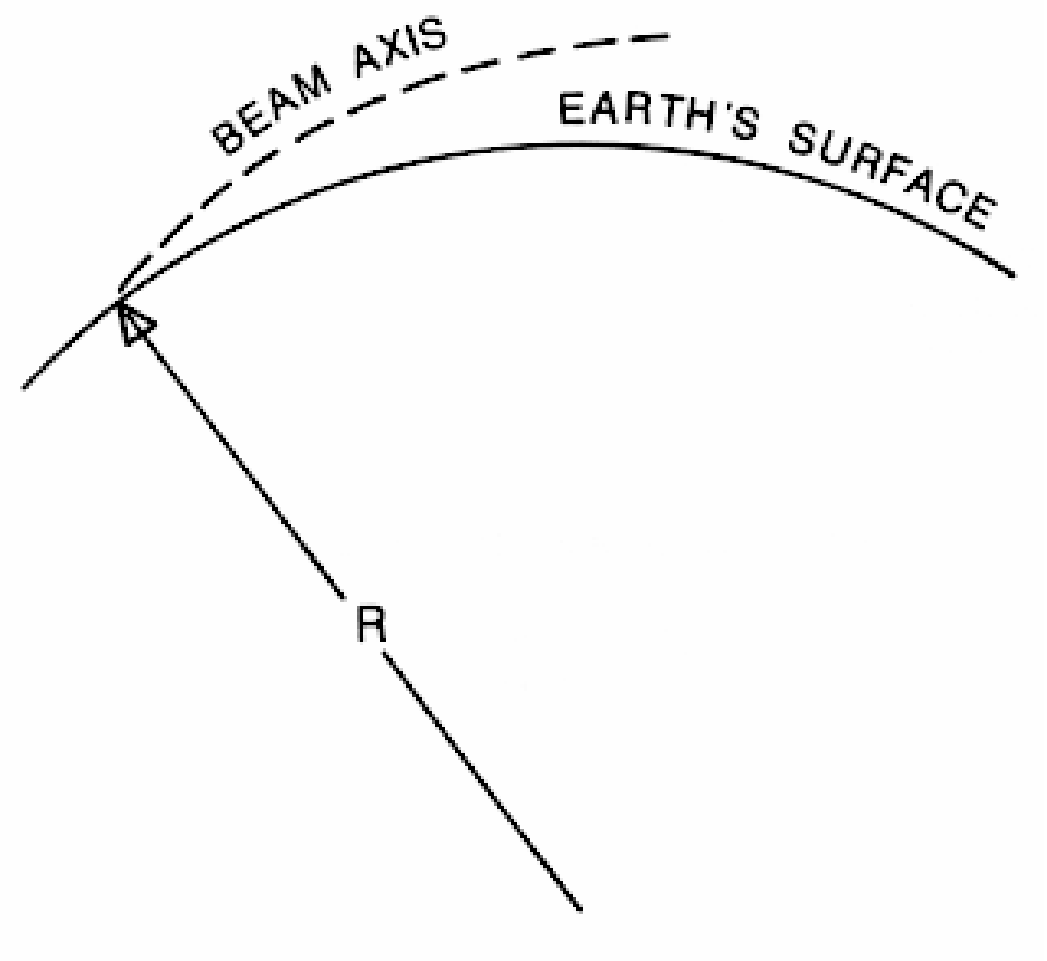

Figure 3-11
Beam Propagation Path Due to Refraction

Assuming standard atmospheric conditions, the nominal radar beam axis is schematically illustrated.

A similar approach to height determination is the use of nomograms such as the one given in Figure 3-12. Nomograms such as this account for the mean Earth curvature but not local terrain variation and assume a constant linear decrease of the refractive index with height.

A more rigorous model of the refractivity height function has been developed by the National Bureau of Standards, Central Radio Propagation Laboratory (CRPL).

The normalized refractive index, as a function of height in this model, is given by: $N = N_s \exp[-c_e(h-h_s)]$ where N_s and c_e are constants and h_s is the surface or initial height. This is referred to as the CRPL exponential reference model. The constants may be specified from surface refractivity. Values of $N_s = 313$ and $c_e = 0.1439$ are average values for the United States.

The differences in heights predicted by the 4/3 Earth or linear refractive index vertical gradient and the exponential gradient are usually negligible for the WSR-88D, i.e., small compared to radar beam dimension at the ranges of interest. A comparison of heights based on the two models is tabulated in Table 3-2.

Table 3-2
Height Based on Exponential Minus Height Based on 4/3 Earth Curvature

Elevation Angle	Slant Range 185 km/100nm		Slant Range 370 km/200nm	
	meters	feet	meters	feet
0	30	100	366	1200
0.5	61	200	610	2000
1.0	91	300	793	2600
2.0	152	500	1128	3700
4.0	244	800		
Radar two-way beam width	2257	7400	4511	14800

Ranging errors due to beam bending are also usually negligible (small compared to sample volume depth, Appendix A). This is shown in Figure 3-13 based on the CRPL model.

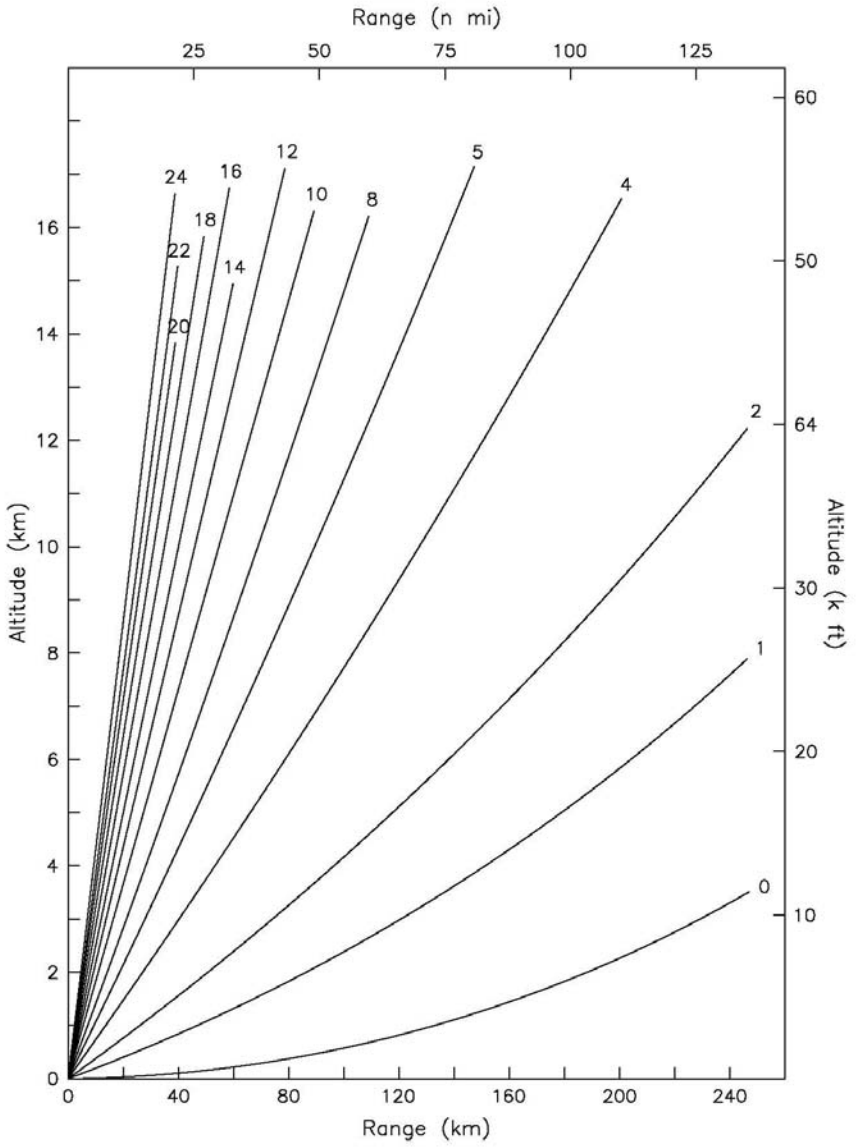

Figure 3-12
Range-Radar Beam Altitude Nomogram

(Standard Atmosphere)

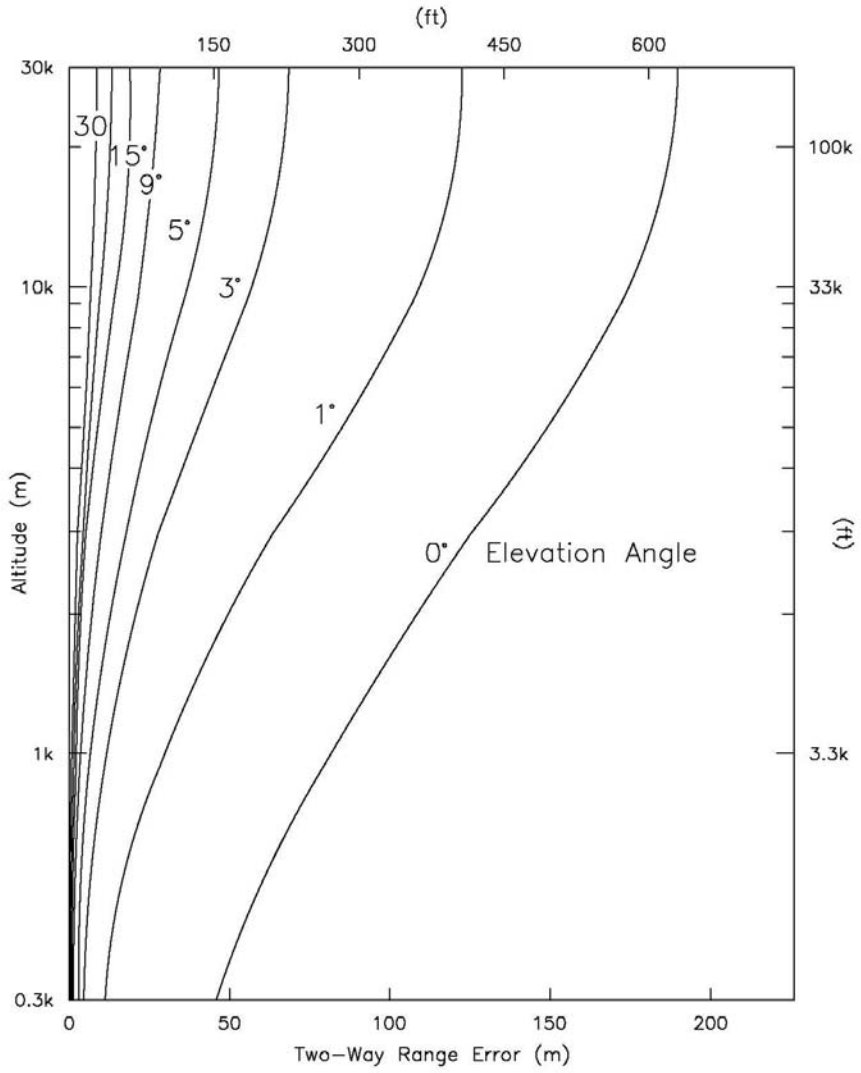

Figure 3-13
Range Error

Range error as a function of echo altitude and elevation angle due to beam bending in a standard atmosphere (CRPL model).

3.4.2 Anomalous Propagation. Normal atmospheric propagation conditions, however, may not be present at all times. In some cases the temperature may first increase with height and then decrease (temperature inversion), or the moisture content of the atmosphere may decrease very sharply close to the Earth's surface, or a combination of these atmospheric variations may occur such as to substantially perturbate the standard refractive index-height dependency. These anomalous conditions may modify the atmosphere in such a way as to provide a "duct," or propagation path, whereby the radio waves are bent substantially more than in the standard atmosphere and, in some cases, bent enough to intercept the Earth's surface. (While sub-refraction [beam bending less than standard] also occurs in the atmosphere, that condition does not result in anomalous propagation and is not treated here.)

In radio wave propagation work, the characteristic used to predict the probable degree of bending of the radio wave is the modified index of refraction curve. The modified index of refraction, M, combines the refractive index contribution from pressure, temperature, and moisture into an index-height relationship and subtracts this relationship from the standard atmosphere index-height relationship. Thus, M provides a measure of beam bending relative to the standard propagation.

Examples of temperature and specific humidity height distribution and the associated curves are given in Figure 3-14. Curve A is the distribution for the standard condition. Curves B, C, and D illustrate conditions under which anomalous propagation (AP) is likely to occur.

The condition shown in B is the most common duct-producing situation and is usually the result of one of the following meteorological conditions:

- Nocturnal radiation causing a temperature inversion near the ground and a sharp decrease in moisture with height.

- A flow of warm moist air over cooler surfaces, especially water, resulting in a cooling of the air in the lower layers and the addition of moisture.

- A diverging downdraft under a thunderstorm resulting in a temperature inversion in the lower few thousand feet as the cool air spreads out from the base of the storm. This is infrequent but can be very important because of its proximity to the storm.

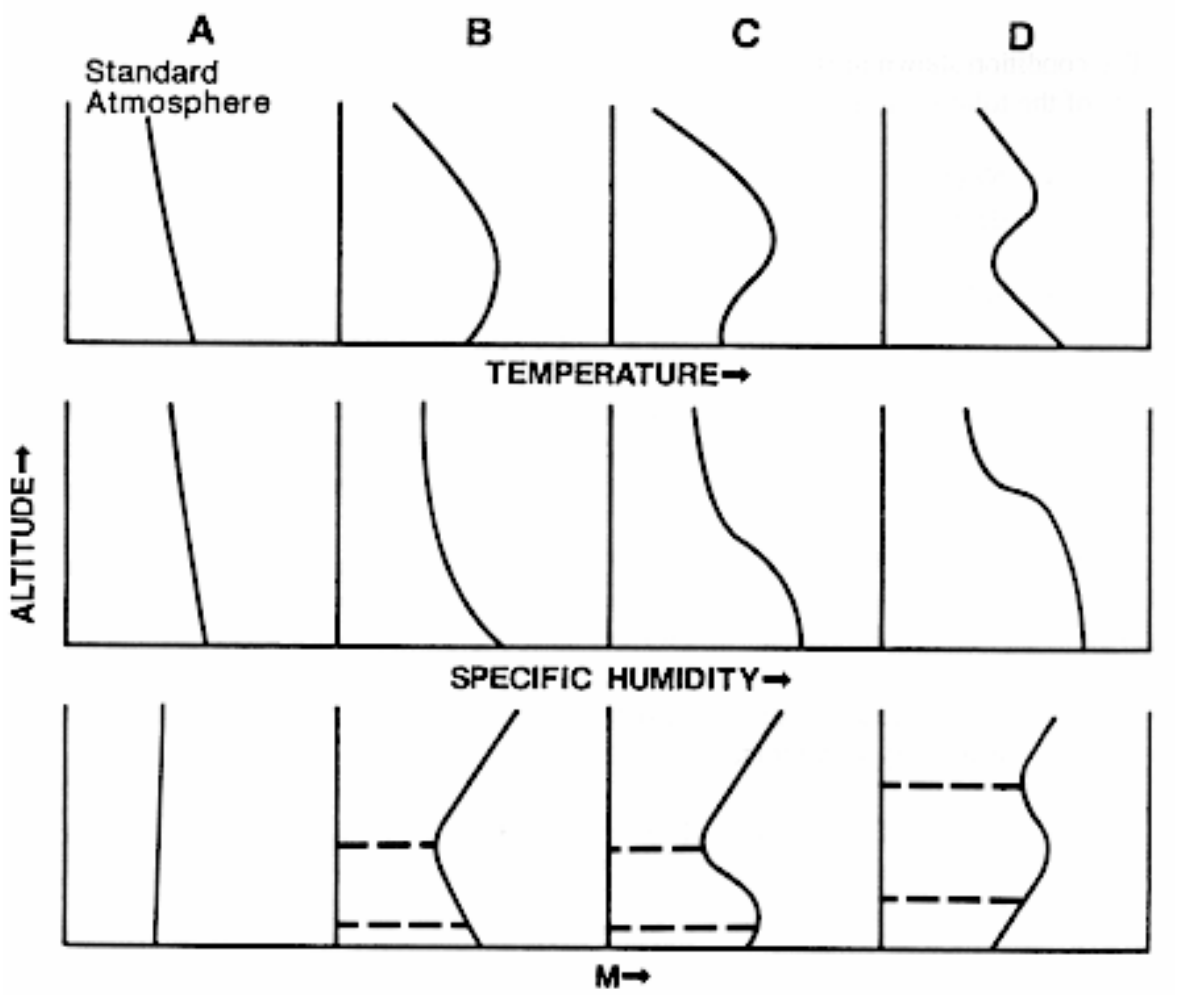

Figure 3-14
Meteorological Conditions Likely to Result in Anomalous Propagation

M is the modified index of refraction or deviation of beam bending from that under standard conditions. The duct, where ducting occurs, is shown by dashed lines. See text for a description of the meteorological conditions that can produce the profiles shown in B, C, and D.

Conditions shown in Curve C are less frequent than those shown in B and are sometimes associated with a low-level inversion through which the specific humidity decreases sharply. Meteorological conditions that can produce these are:

- A subsidence inversion close to the ground especially when the air close to the ground is initially very moist.

- A flow of warm moist air over a cool body of water by turbulent winds. Turbulence can cause the inversion to be lifted above the surface and a nearly adiabatic lapse rate in the lower layers.

The ducts shown in B and C occur at low levels and are of most concern to ground-based radars such as the WSR-88D. Conditions shown in Curve D result in an upper-level duct that seldom result in sufficient bending of the beam to cause interception with the Earth's surface. This is, however, a source of antenna pointing error.

The anomalous signal return is from the Earth's surface and, therefore, has statistical properties very similar to the normal clutter return. The significant differences in the normal clutter and the anomalous clutter signals are a slightly larger width and smaller reflectivity values associated with the anomalous signal. Generally, the AP will be removed by the ground clutter suppressor if the suppressor is active in the AP region. Activation of the suppressor may require manual intervention since AP will normally occur outside the ground clutter map.

Radar signals or echo properties that can be used to identify AP (in conjunction with knowledge of the meteorological situation conducive to the occurrence) are:

- Small temporal variability of the echo in reflectivity, velocity, and spectrum width.

- Large irregular areas of zero velocity.

- A larger number of small-scale features, particularly high-intensity cores in the reflectivity field.

- Vertical variability.

- Large reflectivity gradients, i.e., $dZ/d(r,\theta) > 20$ dB km^{-1}.

- Large gradients in the spectrum width field.

Occurrence of these features should be used in the decision to activate the intensity and Doppler suppressors, in the region outside the clutter map.

3.5 Signal Attenuation.

3.5.1 Atmospheric Attenuation. Any atmosphere, standard or non-standard, is an attenuating medium at a 10 cm wavelength. In the clear atmosphere, an incident frequency of 3 GHz is well below the attenuation resonances associated with water vapor (first maxima at f $\simeq$ 23 GHz) or oxygen (first maxima at f $\simeq$ 62 GHz) but even the small attenuation associated with this wavelength can accumulate to significant values over the maximum range coverage of the WSR-88D.

Two-way attenuation by the International Civil Aviation Organization (ICAO) standard atmosphere is shown in Figure 3-15 and is accounted for in the WSR-88D signal intensity calculation.

Primarily due to oxygen and water vapor, the loss, L, (where L_a is the total loss) as a function of elevation angle, ϕ_e, is given approximately by:

$$L_a \cong L(\phi_e)\left[1 - \exp\left[-\frac{r}{r(\phi_e)}\right]\right]$$

$$L(\phi_e) = 0.4 + 3.45 \exp\left[-\frac{\phi_e}{1.8}\right]$$

$$r(\phi_e) = 27.8 + 154 \exp\left[\frac{\phi_e}{2.2}\right]$$

For λ =10 cm and r <200km (108 nm), ϕ_e <10°, the above approximates the theoretical loss to within 0.2 dB.

3.5.2 Rainfall Attenuation. Signal attenuation due to rainfall is generally less than 1 dB and is accounted for in the WSR-88D.

For a temperature of 0°C and a modified Marshall-Palmer drop-size distribution, the two-way attenuation, K_p, at λ = 10 cm is given by:

$$K_p = 6(10^{-5})\, Z_e^{0.62} \text{ dB km}^{-1}$$

and shown graphically in Figure 3-16.

Two-way attenuation will exceed 0.1 dB km^{-1} at reflectivity greater than 53 dBZ and, on occasion, the total attenuation can exceed several dB. Any correction for this effect must be made subjectively by the user.

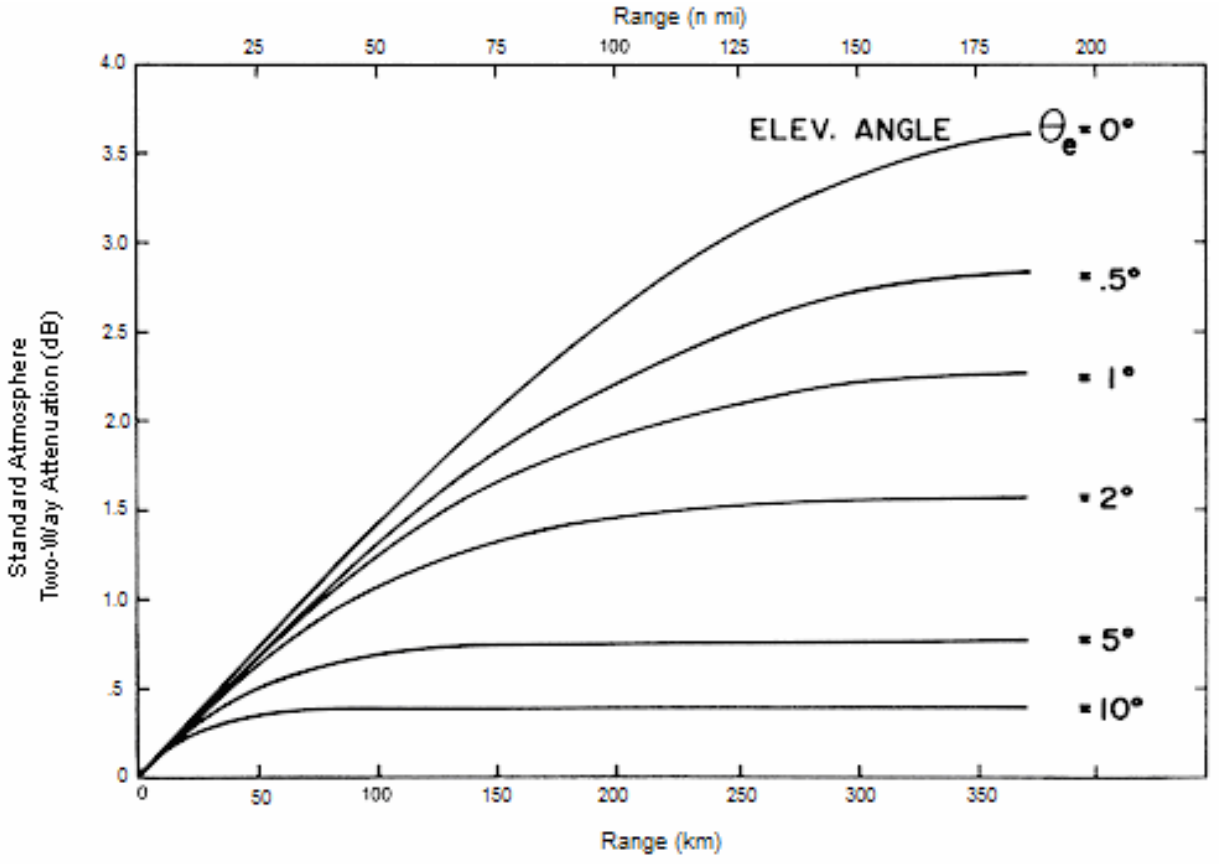

Figure 3-15
WSR-88D Signal Attenuation by the ICAO Standard Atmosphere

This attenuation is accounted for in the radar reflectivity estimate.

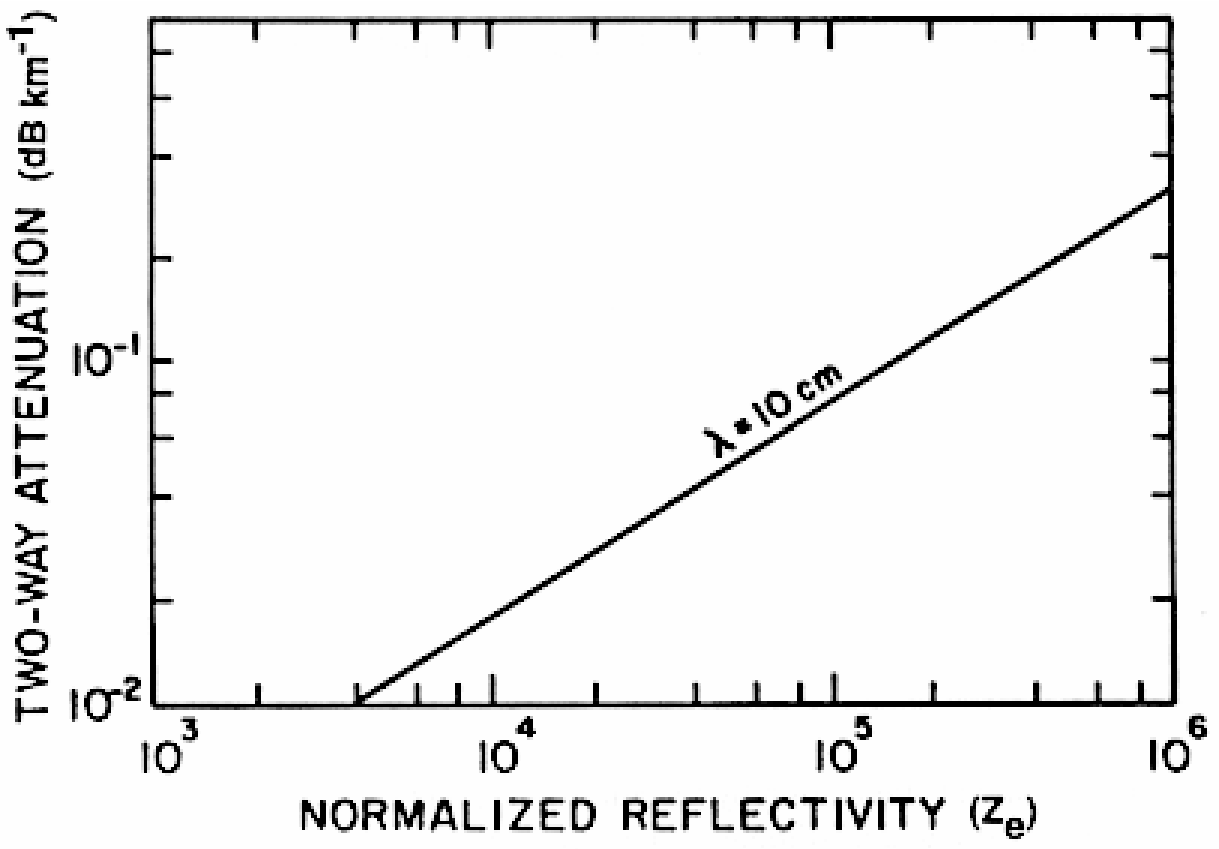

Figure 3-16
Attenuation of a 10 cm Signal by Rainfall

This attenuation is accounted for in the WSR-88D. For reflectivities greater than 53 dBZ, the user must subjectively make the correction.

3.5.3 Lack of Beam Filling. Another phenomenon, which is not attenuation but that also results in an underestimation of reflectivity, is the lack of beam filling, i.e., an apparent Z_e range dependency other than r^{-2}. (Recall that Z_e is interpreted as a volume reflectivity assuming homogenous reflectivity in the sample volume.) The effect can be visualized as an increase in the range exponent. The overall or average effect for a large number of situations is shown in Figure 3-17 for storms in the southern Great Plains. Although small scale meteorological features can fail to fill the horizontal dimension of the beam at the longer ranges, the predominant effect is the failure to fill the beam in the vertical.

The magnitude of underestimation is highly dependent on the particular meteorological situation and is usually more significant for non-convective precipitation systems, having low echo tops, than for convective storms.

In summary, signal attenuation by the atmosphere and rainfall or lack of radar beam filling all cause a systematic underestimate of the true signal strength. Attenuation by the atmosphere, usually the most appreciable effect, and attenuation by rainfall are objectively accounted for by the WSR-88D.

3.6 Data Contamination by Antenna Sidelobe Signal. An occasional source of data contamination is simultaneous reception of signals at comparable power levels through both the antenna pattern main lobe and its sidelobes. This occurs when the meteorological reflectivity gradient exceeds the two-way sidelobe/main lobe isolation.

Antenna sidelobe levels of the WSR-88D are described as follows:

> In any plane, the first sidelobe level is less than or equal to -27 dB relative to the peak of the main lobe. In the region between $\pm$2 and $\pm$10 degrees from the axis of the main lobe, the sidelobe level shall lie below a straight line connecting -29 dB at $\pm$2 degrees and -34 dB at $\pm$10 degrees. Between $\pm$10 degrees and $\pm$180 degrees the sidelobe envelope is less than or equal to -40 dB relative to peak of the main lobe.

These blanket criteria, along with a typical actual performance, are shown in Figure 3-18. Generally, the actual pattern is about 5 dB below the prescribed envelope in the region beyond $\pm$2 degrees. Other characteristics of interest that are frequency dependent and vary across the operational band include:

- first sidelobe maximum is at about +1.5 degrees from the main lobe axis.
- first null is at about $\pm$1.2 degrees.
- sidelobe periodicity is about 1.23 degrees.

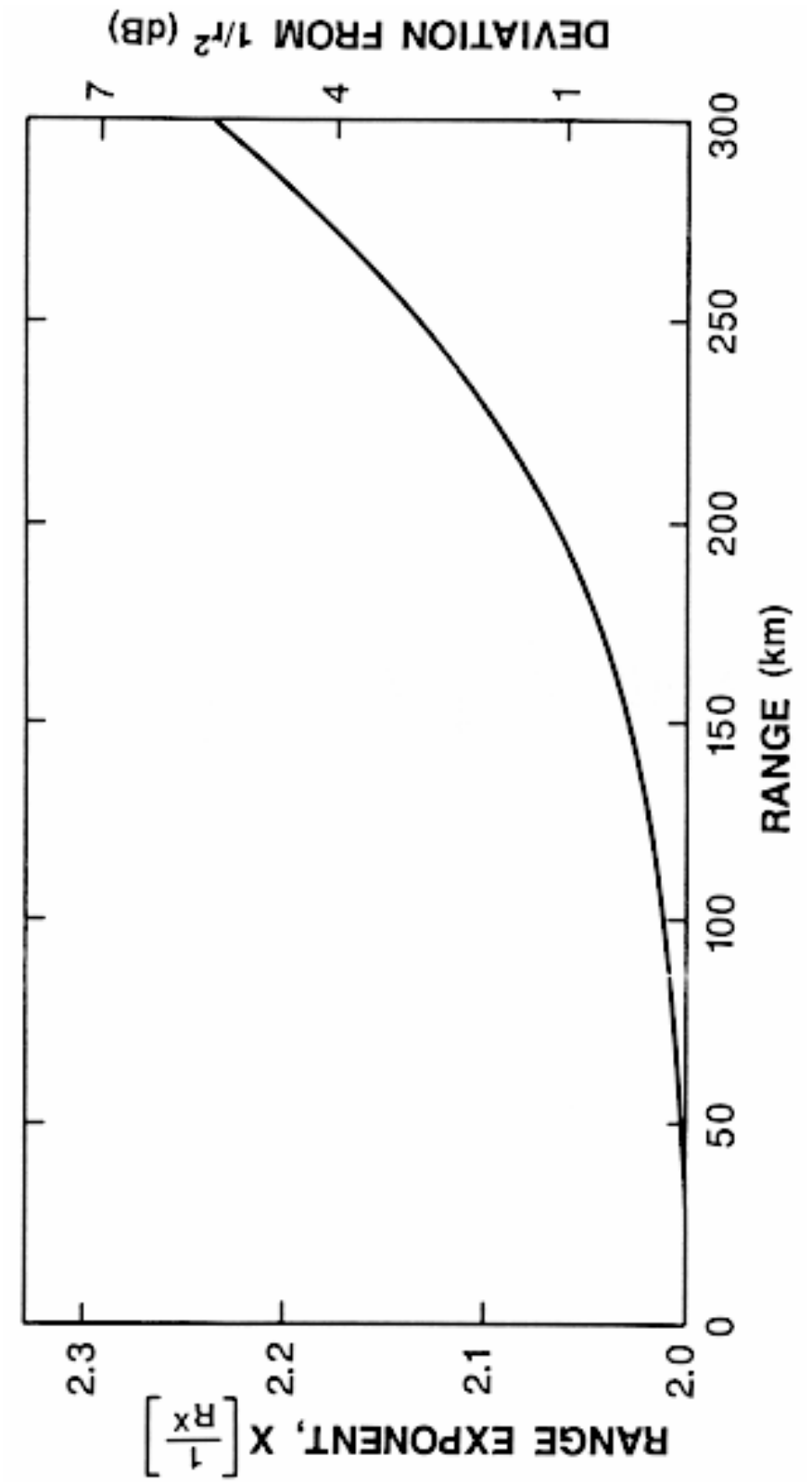

Figure 3-17
Deviation in Apparent Range Dependency of Z_e Due to Lack of Radar Beam Filling

Results shown are an empirical derivation for storms in the southern Great Plains and not valid for general application.

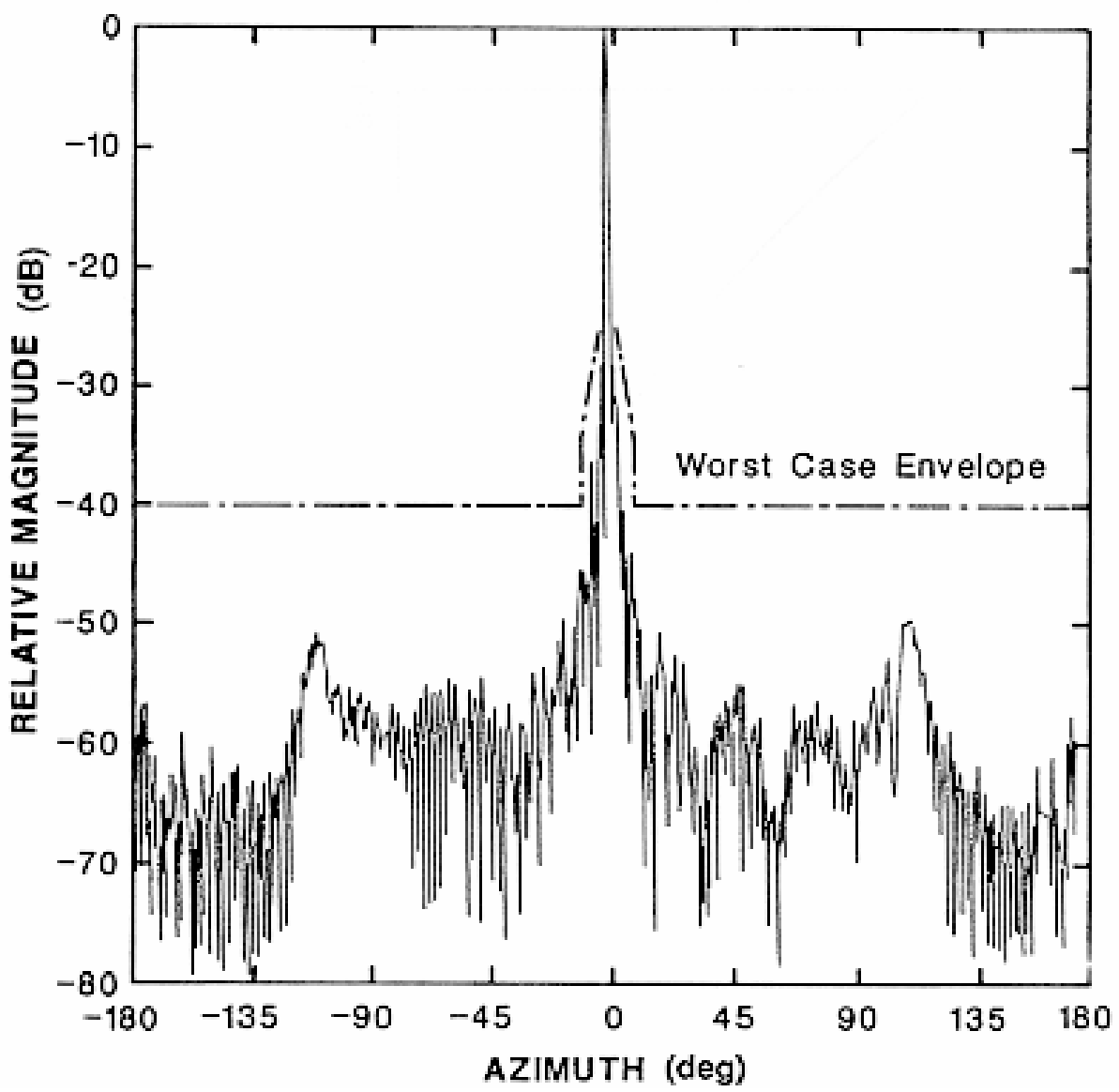

Figure 3-18
Typical Antenna Pattern for the WSR-88D and
Worst Case Sidelobe Envelope

Generally the sidelobe level is several dB below the envelope.

The two dimensional antenna pattern is given by the revolution of the pattern in a plane about the beam axis with the addition of the perturbations in sidelobe level due to antenna aperture blockage by non-symmetry of the feed and support spars. While the main lobe illuminates a circular region of space, the sidelobes illuminate an annulus and the sidelobe signals can originate from any portion or this entire region.

Conditions under which sidelobe detection will occur can be predicted from the known two-way antenna pattern. For example, in order to detect a signal through the first sidelobe, at signal strength equal to that detected through the main lobe, the reflectivity of the meteorological signal in the sidelobe (i.e., 1.2 degrees from the main lobe) must be stronger than the signal in the main lobe, by at least the two-way, first-sidelobe isolation (i.e., >50 dB). This requires a reflectivity gradient of greater than 50 dB per 1.2 degrees (greater than 40 dB degree^{-1} sustained over about 2 degrees). This is a rather large value and seldom-encountered in practice. However, at 6 degrees from the main lobe, the pattern envelope ensures that the sidelobe level is only 30 dB which, under the above criteria, requires a gradient of about 10 dB degree^{-1} sustained over about 6 degrees. Severe convective storms can occasionally support gradients of this magnitude. Beyond 10 degrees the sidelobe level is less than 40 dB with an isolation of 80 dB. As with the first sidelobe, meteorological signal coupling through these higher order sidelobes is rare.

From the prescribed envelope, the worst-case condition for signal detection through the antenna pattern sidelobes can be specified in terms of the reflectivity difference subtending a given angle. This is shown in Figure 3-19. In the use of this graph, it should be remembered that the actual antenna sidelobe level is probably several dB lower than the "worst-case envelope" and, therefore, the reflectivity difference required for coupling is several dB greater.

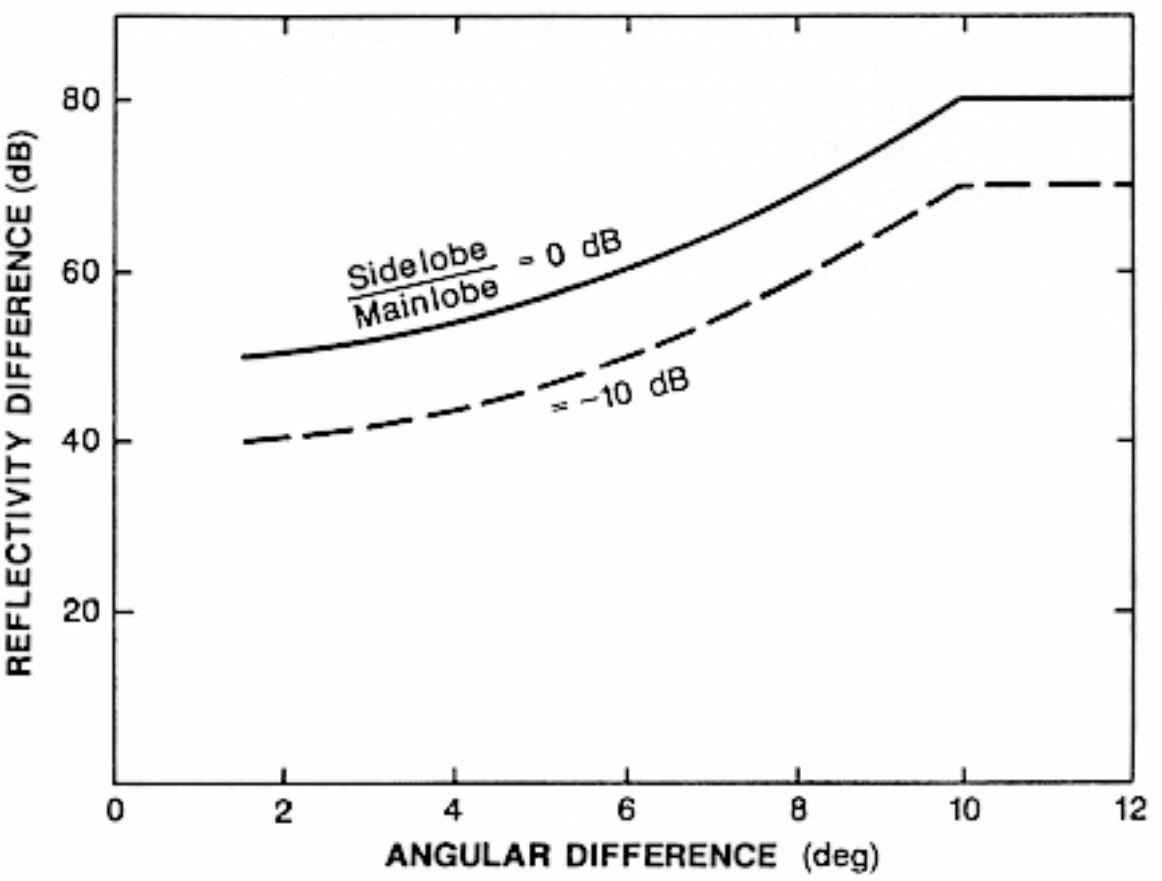

Figure 3-19
Reflectivity Difference and Angle Subtended Necessary for Signal Contamination Through Sidelobe Coupling

The ratio $\frac{\text{Sidelobe}}{\text{Main lobe}}$ is the relative power.

REFERENCES

Battan, L J., 1973: *Radar Observations of the Atmosphere*. Univ. of Chicago Press, Chicago, IL, 323 pp.

Baxter, T. L., 1966: An empirical determination of the WSR-57 radar range attenuation function for Oklahoma thunderstorms. Preprints, *12th Conference on Radar Meteorology*, Amer. Meteor. Soc.

Chrisman, J. N. and C. A. Ray, 2005: A first look at the operational (data quality) improvements provided by the Open Radar Data Acquisition (ORDA) system. Preprints, 3*2nd Conference on Radar Meteorology*, Albuquerque, NM, Amer. Meteor. Soc., paper P4R.10.

Doviak, R. J., and D. S. Zrnic', 1984: *Doppler Radar and Weather Observations*. Academic Press, Inc., Orlando, FL, 458 pp.

Johnson, J. C., 1962: *Physical Meteorology*. John Wiley & Sons, Inc., New York, NY, 393 pp.

Kerr, D. E., 1951: *Propagation of Short Radio Waves*. McGraw Hill Book Co., New York, NY, Chapter 7, 710 pp.

Marshall, J. S., and H. Hitschfeld, 1953: Interpretation of the fluctuating echo from randomly distributed scatterers, Part I., *Can. J. Phys.,* **31***,* 962-994.

Nathanson, F. E., 1969: *Radar Design Principles*. McGraw Hill Book Co., New York, NY, Chapter 6.

Skolnik, M. I., 1970: *Radar Handbook*. McGraw Hill Book Co., New York, NY, pp. 2-51 to 2-59.